Journal Pre-proof

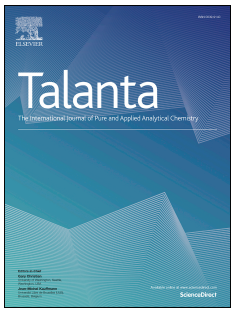

Vegetable waste Scaffolds for 3D-stem cell proliferating systems and low cost Biosensors

Rocco Cancelliere, Francesca Zurlo, Laura Micheli, Sonia Melino

PII: S0039-9140(20)30962-0

DOI: https://doi.org/10.1016/j.talanta.2020.121671

Reference: TAL 121671

To appear in: *Talanta*

Received Date: 2 August 2020

Revised Date: 10 September 2020

Accepted Date: 14 September 2020

Please cite this article as: R. Cancelliere, F. Zurlo, L. Micheli, S. Melino, Vegetable waste Scaffolds for 3D-stem cell proliferating systems and low cost Biosensors, *Talanta*, https://doi.org/10.1016/j.talanta.2020.121671.

Graphical Abstract

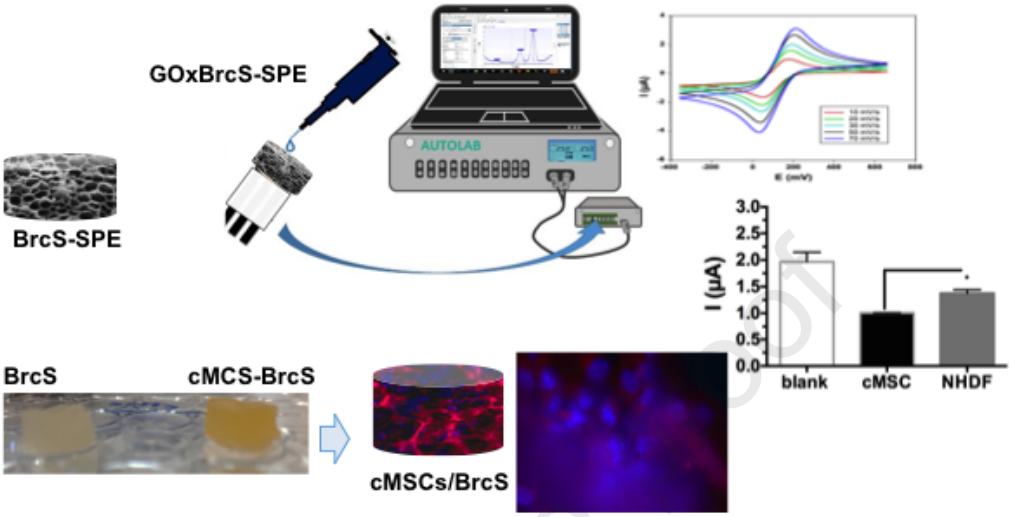

Vegetable waste Scaffolds for 3D-stem cell proliferating systems and low cost Biosensors

Rocco Cancelliere[1], Francesca Zurlo[1], Laura Micheli[1&]* and Sonia Melino[1,2&]*

[1.] Department of Chemical Science and Technologies, University of Rome "Tor Vergata", via della Ricerca Scientifica 1, 00133-Rome, Italy;
[2] CIMER Center for Regenerative Medicine, University of Rome Tor Vergata, via Montpellier 1, 0166-Rome, Italy;
[&] These authors contributed equally to the work
* Correspondence: Sonia Melino e-mail: melinos@uniroma2.it; Laura Micheli e-mail: laura.micheli@uniroma2.it; Tel. #39-067259-4410/4420;

Abstract

Vegetable wastes represent an inexpensive and sustainable source of valuable bioproducts for several applications. Natural micro-porous and fibrous materials can be obtained from a very cheap and abundant cellulosic bio-waste. Here we demonstrated that vegetable waste derivatives can be suitable as scaffolds for biosensors and 3D cell growth. Many studies have been addressed to fabricate biocompatible 3D scaffolds for mammalian stem cells cultures and develop novel systems able to reproduce the complexity of the *in vivo* microenvironment. Many of these products are proprietary, expensive or require chemical synthesis. The recycling and revaluation of vegetable derived tissues to fabricate scaffolds for analytical biosensors 3D stem cell cultures platforms may represent a very low-cost approach for toxicological and environmental analyses. In this approach, potential applications of vegetable-derived tissue for biosensing and 3D stem cell cultures were investigated. Micro-structured scaffolds from stalk of broccoli, named BrcS, were either functionalized for production of enzymatic 3D-biosensors or preconditioned to be used them as 3D-scaffolds for human mesenchymal stem cells cultures. The conditions to fabricate 3D-biosensors and scaffolds for cell growth were here optimized studying all analytical parameters and demonstrating the feasibility to combine these two properties for an innovative solution to ennoble vegetable wastes.

Keywords: cellulose scaffold, glucose oxidase, biosensor, 3D- stem cell cultures, MSCs, cell proliferation assay.

1. Introduction

One of the main criteria for an ecological sustainability is that the waste generation should not exceed the assimilative capacity of the environment. Large amounts of co-products, by-products and bio-wastes are generated from the processing of vegetables and fruit and currently they are not properly managed both in environmental and economic terms. However, these bio-wastes can be an inexpensive source of valuable bio-products and bio-energy.

Research on the reuse and renewal of the waste products together with the improving of the waste management could lead to increase opportunities to exploit the bio-wastes resulting in reducing environmental impact and enhancement of competitiveness through the production of new bio-products at lower cost. Thus, the exploration of natural resources, as sustainable precursors, provide a family of "green materials" with several and different applications from engineering to medicine. For instance, the development of novel micro-structured biomaterials to create three-dimensional (3D) cell culture systems suitable for preclinical studies on drugs, cytotoxicity analyses and tissue regeneration has gained traction in recent years [1–7]. The development of novel systems able to reproduce the complexity of the i*n vivo* microenvironment mimicking the biochemical and physical properties of the extracellular matrix (ECM), which has a significant impact on numerous critical physiological and pathological processes, opens relevant questions about the production of 3D micro-structured scaffolds. [1] Although 3D-printing technology allows to accurately fabricate 3D structures, it is not easy to create scaffolds with a manifold microvasculature as well as in the plants using biocompatible polymers.

Cellulose derived from plants or bacteria is a biocompatible material, which has been also studied for several clinical applications and biosensing [8,9] such as to promote wound healing. [10,11] Apple-derived cellulose scaffolds have been used as implantable and biocompatible porous cellulose scaffolds for 3D culture of mammalian cells. [12,13] Recently, further, the osteoblastic differentiation of human mesenchymal stem cells and iPSCs has been demonstrated in cellulose-porous based scaffolds and explored the clinical prospective for *in vivo* implants. [14–16] Several types of cell lines, such as human endothelial, mesenchymal and pluripotent stem cells have been used for recellularizing plant-derived scaffolds that either colonized

the inner surfaces of plant vasculature and the outer surfaces of plant scaffolds preserving their functional properties. [2]

3D cell culture promises to more closely reflect the biochemical and physical properties of the cellular microenvironment found in tissues and organs [8,10], and so the development of novel sustainable biomaterials towards this effort is of considerable importance. Physiologically relevant 3D cell culture models are ideally suited to bridge the gap between conventional 2D preclinical models and *in vivo* clinical studies in humans. Several 3D cell culture models have the potential to improve the predictive outcome of preclinical toxicity studies and could be preclinical models able to better recapitulate pathophysiological processes underlying diseases of specific tissues and organs in humans. Microfabrication and microfluidics technologies have been used to generate several miniaturized 3D on-chip-models of organs with *in vivo*-like functionality, which may be very useful for toxicity testing. [17] Many 3D assays can be cumbersome, technically challenging, and may require highly specialized and uncommon detection methods. Nerverthless, the cost of some 3D cell culture systems can be prohibitively high and hinder their use for drug discovery or toxicity testing. These limitations, however, are progressively and mindfully being overcome thanks to emerging technologies and improved 3D *in vitro* assays. Recent studies have shown that the development of analytical biosensing devices using cells cultured on sustainable 3D scaffolds as biocatalyst and transducer, are able to convert a biological or biochemical signal into an electrical or optical signal. [18,19] These new tools could represent a very suitable mode for sensing and accurately predicting physiological responses to therapeutic or toxic compounds. In this study we used a natural waste-biomaterial derived from stalk of broccoli for the fabrication of low-cost broccoli 3D-scaffolds (BrcS). BrcS were here used as micro-structured and functionalized material for 3D adult stem cells cultures and enzymatic immobilization for biosensors development, providing a proof of concept for potential combined approaches.

2. Materials and Methods

2.1 BrcS preparation

The stalk of broccoli (Brc) was cut in slides with a thickness of 0.2 cm and treated using the protocol described in materials and methods. The Brc-slides were incubated

for 24h in a decellularization buffer solution with 0.5% of sodium dodecyl sulfate (SDS) with magnetic stirring at room temperature (23°C). After this decellularization process the slides were washed in H_2O_{dd} for several times in order to remove the decellularization buffer and were lyophilized and stored in dried condition at room temperature.

2.2 Water uptake of BrcS

Water uptake study was performed to determine the water holding capacity (permeability) of BrcS. Briefly, scaffolds were immersed in distilled water at two different temperatures (4°C, 25 °C), for various time periods namely 0 hr, 3hr, 5hr and 24hr. After different time intervals, the samples were removed from water and weighed. The water uptake of the matrices was calculated by the following equation (eq.1) [20,21]:

$$\text{Water Uptake } \% = \frac{W_{wet} - W_{dry}}{W_{wet} + W_{dry}} \times 100 \qquad \text{eq.1}$$

where W_{wet} and W_{dry} are the weight of the wet matrix and the dry matrix, respectively.

2.3 Scanning Electron Microscopy (SEM) of BrcS

BrcS were characterized using a field emission gun scanning electron microscope (FEGSEM, Cambridge Leo Supra 35, Carl Zeiss). The samples were frozen in liquid nitrogen and then fractured. The fragments were placed on carbon tape and sputter-coated with gold under argon atmosphere (25 mA, 120 s). Specific imaging detectors were chosen accordingly.

2.4 Attenuated total reflection Fourier transform infrared spectroscopy (ATR-FTIR) of BrcS

FT-IR analysis of BrcS was performed with a FT-IR spectrometer (Jasco, FT/-6600) equipped with an attenuated total reflectance (ATR) cell. Spectra were recorded by placing and pressing the samples into contact with the ATR cell, in the following conditions: wavenumber ranged from 500 to 4500 cm^{-1}, with a spectral resolution of 4 cm^{-1} and 32 scans.

2.5 BrcS Biosensors preparation

All chemicals from commercial sources and solutions were of analytical grade. Glucose oxidase (GOx) from *Aspergillus Niger* (181 U/mg), ferric chloride, potassium ferricyanide, glutaraldehyde, hydrogen peroxide, Nafion®117 and D-glucose (Sigma-Aldrich, Italy). Buffer solutions used are 50 mM phosphate buffer, pH 7.4, with 10 mM KCl, and only 100 mM KCl at pH 6. The glucose test solution was prepared by using 50 mM phosphate buffer, pH 7.4, with 10 mM KCl, and 0.1% of Kathon^{TM} CG solution added as microbial preservative.

Screen Printed Electrodes (SPEs) were home-produced with a 245 DEK (High performance multi-purpose precision screen printer, Weymouth-UK) screen-printing machine. Graphite-based ink (Elettrodag 421) from Acheson (Milan, Italy) was used to print the working and the counter electrode. The SPE support was a folding polyester film (Autostat HT5) obtained from Autotype Italia (Milan, Italy). The electrodes were produces in foils of 48. The diameter of the SPE working electrode was 0.3 cm resulting in an apparent geometric area of 0.07 cm^2. A silver ink was used to print the reference electrode (Acheson Elettrodag 4038 SS). The application of an insulating print (Argon Carbonflex 25.101S) defines the actual surface area.

Cyclic voltammetry (CV) and amperometry were performed using an Autolab electrochemical system (Eco Chemie, Utrecht, The Netherlands) equipped with PGSTAT-12 and GPES software (Eco Chemie, Utrecht, The Netherlands).

2.6. BrcS-SPE preparation

The SPEs were modified with broccoli tissues following a multi-step procedure. Initially, the BrcS were soaked in a solution of distilled water (3 hours). After that, broccoli tissues were positioned to cover the electrode surface of the SPEs and subjected to dehydration at 37°C for 120 min. The platforms (BrcS-SPE) were therefore ready to be rehydrated (70 µL of working solution) and to be subjected to electrochemical measurement.

The diffusion coefficient (D_0), reported in Table 2, was calculated using Cottrell Equation (eq. 2) [22]:

$$I_p = (0.4463)nFAC\sqrt{\frac{nF\nu D_0}{RT}} \qquad \text{eq.2}$$

where F is the Faraday constant ($C \cdot mol^{-1}$), R the universal gas constant ($J \cdot K^{-1}mol^{-1}$), n is the number of electrons exchanged, A the electrodic surface (cm^2), C is the analyte concentration ($mol \cdot cm^{-3}$), D_0 is the diffusion coefficient ($cm^2 \cdot s^{-1}$) and ν is the scan rate ($mV \cdot s^{-1}$), respectively.

2.7 GOxBrcS-SPE preparation

The working electrode was modified with Prussian Blue using a chemical procedure already optimised in a previous work [19]. Glucose biosensors were obtained by immobilising GOx onto Brc-tissue (GOxBrcS-SPE). In particular, the BrcS were soaked in a solution of GOx (10 $mg \cdot mL^{-1}$), Nafion (2%), Glutaraldehyde (10%) e BSA (5%) in distilled water (3 hours).

After that, broccoli tissues are positioned to cover the electrode surface of the SPEs and subjected to dehydration at 37 ° C for 2 hours. The platforms (GOxBrcS-SPE) are therefore ready to be rehydrated (70 µL of different concentration of glucose solution) and to be subjected to electrochemical measurement (Figure 1).

The enzymatic kinetic parameters were obtained using the linearization of Lineweaver-Burk expressed by equation (2) [23,24]:

$$\frac{1}{I} = \frac{1}{I_{max}} + \frac{K_M^{app}}{I_{max}[S]} \qquad \text{eq.3}$$

where [S] is the concentration of the substrate, I is the cathodic current at -0.05V, K_M^{app} is the apparent Michaelis-Menten constant for the enzymatic reaction and I_{max} is the steady-state current.

The Hill coefficient (h) was calculated by the log[I/(Imax-I)] *vs.* log [S] plot, where [S] was the substrate concentration.

The measurements were performed using 0.01 mM glucose solution in 50 mM phosphate buffer, pH 7.4, with 10 mM KCl.

2.8. Cell glucose-uptake analysis and Stem cell proliferation on BrcS

Cell studies were performed using normal human dermal fibroblasts (NHDF) and human Lin^- $Sca\text{-}1^{pos}$ cardiac mesenchymal cells (cMSC), which were isolated from human auricular biopsies made during coronary artery bypass surgery and characterized as previously described. [25,26] Both the cell lines were grown using

Dulbecco's Modified Eagle Medium (DMEM) with high glucose concentration (5 $g \cdot L^{-1}$) (Gibco, Italy), containing 10% Fetal Bovine Serum (FBS) (Gibco, Italy), 1% penicillin-streptomycin, 1% L-Glutamine-Penicillin-Streptomycin solution (Sigma-Aldrich, Italy). The experiments of glucose uptake analysis on cells culture medium using GOxBrcS-SPE and GOx-SPE were performed seeding $2x10^3$ cells/cm^2 on Multiwell™ 6-well (Corning™, Italy) for monitoring the growth of both the cell lines and seeding $2x10^4$ cells/cm^2 for the experiments in presence of 100 µM of H_2O_2 as oxidative treatment. The cell growth was monitored by optical microscopy using a Zeiss microscope (Primovert, Zeiss, Italy). After 12 h of cell growth 1 mL of cell culture medium was withdrawn, diluted with 9 mL of phosphate buffer saline (PBS) and analysed by amperometry using the GOxBrcS-SPE and GOx-SPE.

BrcS used as 3D-cell culture systems were washed with PBS and conditioned with culture medium for 2 weeks before seeding.

To assess the stem cells growth onto the BrcS, $40x10^4$ cMSC were seeded onto each BrcS and cultured for two or four weeks in complete medium. The cell viability was investigated by the Water-Soluble Tetrazolium salt (WST-1) assay (4-[3-(4-Iodophenyl)-2-(4-nitrophenyl)-2H-5-tetrazolio]-1,3-benzene disulfonate) (Roche Diagnostics, Sigma Aldrich, Italy). [27]

Nuclei were stained with Hoechst 33342 (Sigma-Aldrich, Italy) by incubation of 4 hours in medium with 50 µL of 1:500 (w/v) Hoechst in 500 µL (total volume) of complete medium without phenol red. Scaffolds were then washed with PBS, fixed with 4% paraformaldehyde (PFA) in PBS for 15 min at room temperature and permeabilized with 0.2% v/v Triton X-100 (Sigma-Aldrich, Italy) for 10 min. Then they were incubated with antibodies specific for α-smooth muscle actin (α-Sma) (Sigma-Aldrich, Italy), followed by the appropriate 488-Alexa fluorochrome-conjugated secondary antibodies (Life Science, Italy), or incubated with 488-Alexa fluorochrome-conjugated phalloidin (Life Science, Italy). Confocal microscopy of the cell-seeded constructs was performed using Nikon Eclipse Ti (Nikon, Japan) and the signal was detected using EZ C.1 software (Nikon).

2.9. Statistical analysis

The cell viability and the molecular analyses were expressed as mean ± standard deviation (SD). All data were analysed using One-way ANOVA test and p values ≤ 0.05 were considered significant.

3. Results and Discussion

3.1 Production and Ultrastructural Characterization of BrcS

Decellularization is commonly employed on vegetable parts to selectively remove cellular components while leaving behind an intact structure. The stalk of broccoli (Brc) was cut in slides with a thickness of 0.2 cm, treated using a decellularization protocol and then from the lyophilized Brc-slides were produced disks with 1 cm of diameter.

The ultrastructural characterization and the physical properties of the vegetables tissue were analyzed. In the Figures 2A and 2B is shown the ultrastructure of Brc-Scaffolds (BrcS) obtained by Scanning Electron Microscopy (SEM).

SEM images show a particular porous and ordered cellulosic structure resembling a honeycomb morphology. BrcS show homogeneous porous structure with porous diameter of 22.17 μm and forming channels, with ordered pipes and network, demonstrating that the preparation of the scaffold does not modify the ultrastructural organization of the vegetable tissue. This morphological characteristic can be of relevant importance for the electrochemical properties and, in particular, for the development of biosensors. [28] The atomic composition of BrcS was analysed by Energy-dispersive X-ray spectroscopy (EDX), and the results are reported in Figure 2C. Noteworthy, the relevant presence of sulphur (S) that could be also related to the high concentration of organosulfur compounds (OSCs) in broccoli. [29]

3.2. Chemical characterization and water-uptake of BrcS

Fourier-transform infrared (FT-IR) spectroscopy was used for the molecular characterization of BrcS and identification of functional groups. The FT-IR spectrum of BrcS (Figure 3A) shows a typical profile of cellulose in the zone between 1,500 and 500 cm^{-1}. [30,31] Three characteristic peaks are present between 1,150 and 950 cm^{-1} ascribed to the vibration and elongation of the hydroxyl –O–H linkages. Moreover, the presence of the peak characteristic of glucosidic units is visible in the area 950–850 cm^{-1}. A wide strip at 3,340 cm^{-1} attributed to the vibration of -OH functions clearly suggests the presence of strong intermolecular hydrogen bonds between cellulose macromolecules. Finally, a band at 2,920 cm^{-1} is characteristic of the vibration of elongation of the methylene ($–CH_2–$) groups.

The % of Water Uptake (% WU) of BrcS was assessed over the time as previously described. [17,18] In the Figure 3B is shown the % WU as a function of time, between 0 and 25 hours at 4 and 37 °C. Despite the different temperatures, the plateau of about 1500 % WU was reached after about 3 hours; therefore 3 h of imbibition time (I.T.) were chosen for the BrcS-biosensor preparation.

3.3 Electrochemical properties of BrcS

BrcS-screen printed electrode biosensor (BrcS-SPE) was realised by hydration of BrcS, applied on SPE, for 180 min with 50 mM phosphate buffer, pH 7.4, directly on the electrode and subsequent dehydration for 120 minutes at 37 °C. An electrochemical characterization of BrcS-SPE was performed by CV in order to evaluate the presence of electroactive compounds able to interfere with the electrochemical measurements. Moreover, the time necessary for an electroactive solution, such as an enzymatic substrate, to arrive on the electrode surface (called scaffold rehydration time - R.T.) for the electrochemical measurement was also assessed. This parameter is relevant in order to develop a biosensor with an immobilized enzyme. The analysis was carried out using 50 mM phosphate buffer, pH 7.4, with 10 mM KCl in the presence and in the absence of Potassium Ferricyanide, $K_3Fe(CN)_6$ (Figure 4), which is the electroactive probe of reference used in CV for its reversible electrochemical behaviour. [32] CVs analysis in only buffer using BrcS-SPE (Figure 4A) showed the absence of electrochemical signal (anodic or cathodic peaks), this indicated the absence of electroactive compounds in Brc-tissue, excluding the possibility of interferences in the electrochemical measurements and promoting BrcS-SPE for biosensing.

The scaffold dehydration time (S.D.T.) was characterized in order to understand the drying time necessary to allow the most stability scaffold-electrode interaction. In this regard, three different S.D.T. times have been studied: 60, 120 and 180 min. This analysis was carried out using a solution of 2 mM Potassium Ferricyanide in 50 mM phosphate buffer, pH 7.4, with 10 mM KCl. The recorded voltammograms of $[Fe(CN)6]^{3-/4-}$ are showed in the Figure 4B) (n = 10, RSD 6%). The better response, in terms of intensity of current were obtained when a dehydration time of 120 minutes was used. The recorded voltammograms of $[Fe(CN)6]^{3-/4-}$ are showed in Figure 4B (n = 10, RSD 6%). Probably, this S.D.T. represents the best

compromise between scaffold dehydration and scaffold-SPE interaction and was used for the broccoli-based sensors.

A little shift of the peak was obsevable, probably due to the micro-heterogeneity of the honeycombe structure between the different BrcS. The ultrastructural variability could lead to little changes of the ferricyanide diffusion, as also demonstrated in other cases by chromatography. [33,34] These little differences between the Brcs do not affect the good quality of the electrochemical data.

The scaffold rehydration time (R.T.) was also defined as the time required for the electroactive species under analysis to reach the SPE interface in order to have the best electrochemical response. In the Figure 4C it is possible to observe that the time (0, 5, 10 and 15 min.) which guarantees the best response in terms of peak current intensity with good repeatability (RSD 7%) is only 5 minutes. Current intensity decreased after 15 minutes probably due to the hydration of the BrcS, The applied rehydration volume was 80 µL and 5 minutes were considered a good agreement between rehydration of the scaffold and diffusion of the electroactive species. The decrease of the faradic peak current, observed at 15 minutes in Figure 4C, could be due to the capillarity phenomenon in the 3D structure of the BrcS that leads to decrease the amount of the solution that reach on the electrode interface. A similar decrease of the current peak over time was also previously described using other systems [35,36]. Furthermore, the relative peak currents and redox potentials are shown in Table 1.

After analytical characterization of BrcS-SPE more detailed study about its electrochemical behaviour has been carried out using current and potential obtained by CVs. In particular, the diffusion coefficient (D_0) are reported in Table 2, and the corresponding voltammograms are shown in Figure 4D. [37] The Anodic (D_A) and Cathodic (D_R) diffusion coefficients (D_O) of ferricyanide, calculated as reported previously using the scan rates of Figure 4D, were then compared with Konopka ($D_O = 7.26 \cdot 10^{-6}$ cm^2s^{-1}) and Mc Duffie ($D_R = 6.67 \cdot 10^{-6}$ cm^2s^{-1}) coefficients. [38] The diffusion coefficients calculated using BrcS based platforms are approximately one order of magnitude lower than those mentioned above. This result can be justified, in the case under study, as ferricyanide probe is contained inside the tissue and needs a certain interval of time to diffuse within the tissue section until it reaches the electrode surface. This type of investigation is important in order to understand how BrcS influences the diffusion processes at the electrode interface.

3.4 Scaffold for electrochemical biosensing

After having carefully characterized all electrochemical parameters, the BrcS-based biosensor selective for glucose (GOxBrcS-SPE) has been studied as an example of the application of Brc as support for enzyme immobilisation. In this regard, the glucose oxidase (GOx), a widely examined and characterized enzyme, was chosen as bio-receptor for the determination of glucose [37,39] to study the application of Brc for biosensing development.

As well known, this enzyme is able to catalyse the glucose oxidation into gluconic acid and hydrogen peroxide, an electroactive compound (Figure **1S)**.

The hydrogen peroxide produced was measured by amperometry, applying a reduction potential of -0.050 V *vs* Ag pseudoreference of SPE. [22,39] The GOxBrcS-SPE platform performances have been compared to the classic glucose sensor GOx-SPE, prepared by a direct immobilisation of the enzyme on SPE, in order to understand the differences that BrcS application entails in terms of stability, detection limit (LOD), working range (WR) and reproducibility (relative standard deviation percentage - RDS%) for the determination of this analyte.

The comparison of the results, reported in Figure 5A and in Table 3, showed that the analytical behaviour of the two platforms, GOx-SPE and GOxBrcS-SPE, for the determination of glucose, are similar, with a slight sensibility for GOx–SPE. In particular, the GOx-SPE and GOxBrcS-SPE sensors, display a linear and stable response in the range from 0.05 to 1.0 µM for glucose with a slope of 0.71 and 0.48 $\mu A m M^{-1}$, respectively. The limit of detection is 12 µM for the classical platform and 16 µM for the BrcS-based devices and correlation coefficient (r^2) is equal to 0.998 and 0.996, respectively (Figure 2S, supplementary materials). These results confirm the possibility to use BrcS for enzymatic immobilization.

A Hill coefficient of 0.99 was calculated for the enzymatic process (r^2=0.998). The finding that the h parameter, calculated from the corresponding Hill's plot, was close to unity, demonstrated that the kinetics of the enzymatic reaction fitted into a Michaelis-Menten type kinetics. [40]

The apparent K_M (Michaelis-Menten constant) were calculated using the Lineweaver-Burk plot (eq.3, Figure 5B) and were of 0.47 ± 0.05 and 0.67± 0.08 for GOxBrcS-SPE and GOx-SPE, respectively. These results demonstrate that GOx-SPE and GOxBrcS-SPE biosensors show a very similar behaviour. Therefore, these data

suggest that in both cases we can have a similar amount of immobilized enzyme and same affinity for the substrate.

3.5 Repeatability and stability of the biosensor

To study the repeatability of GOxBrcS-SPE sensors, amperometric measurements for glucose detection were carried out. In this analysis the same biosensors devices were reused for 10 time with an RSD of 6% for GOxBrcS-SPE.

The stability of the biosensor was studied by monitoring the amperometric response of the same biosensor at regular intervals of 24 hours for 30 days, the biosensor was stored in a refrigerator at 4 °C in dry condition after each analysis. The amperometric responses of GOx/BrcS-SPE platform remained constant in the first 7 days of storage (95% of its initial current response). After this time, the biosensor amperometric response constantly decreased, until 57% of the initial signal in 30 days. The results showed the possibility to have a ready-to -use biosensor with constant current response for a week.

3.6 GOx/BrcS-SPE as sensor for cell culture viability

The GOxBrcS-SPE sensor was used as 3D-biosensor for the analysis of the cell-growth in order to monitor the cellular glucose uptake over the time. Firstly, an analysis of the glucose concentration in the medium of two different cell lines cultures, cMSC and NHDF, was performed after 3 days of cell growth. In Figure **6** are shown the results obtained by analysis of glucose concentration in the medium performed using either GOx-SPE or GOxBrcS-SPE. A lower faradic current was corresponded to a greater glucose uptake. The glucose uptake was extrapolated from the calibration curve where the recorded currents (μA) were reported in function of the concentrations (mM) of glucose ($y=0.714x+0.015$, $r^2=0.998$, and $y=0.482x+0.054$, $r^2=0.996$) for GOx-SPE and for GOxBrcS-SPE, respectively (Figure 3S, supplementary materials). GOx-SPE showed a very similar behaviour, in terms of both repeatability and reproducibility (RSD% 6% and 9%, respectively).

Although the differences in terms of glucose concentration in the cell culture medium were more evident when the analysis was performed using GOxBrcS-SPE, in both the kinds of analyses a major glucose uptake was observed for the cMSC culture medium respect to the NHDF culture medium. The seeding was performed at the same cell

density ($2.5x10^3$ cells/cm^2) for both the cell lines and this result suggests a more active glucose metabolism and/or cell proliferation of cMSC respect to NHDF. This analysis could also open the way to an easy, rapid, not invasive, not expensive and potential real time measurement to identify the differences of metabolism and/or cell proliferation rate between different cell lines.

The ability of GOxBrcS-SPE to assess the cell growth by the glucose uptake was also tested under oxidative stress that was induced by treatment with H_2O_2.

The treatment was performed using 100 μM H_2O_2, which does not significantly interfere with the analysis of the glucose concentration, as shown in the Figure 4S (supplementary material). In the Figure 7 are shown the optical micrographs of cMSC after 12 and 24 h in the absence and in the presence of H_2O_2. The cell culture medium of each sample was analysed using both GOx-SPE and GOxBrcS-SPE biosensors and the results are shown in the Figure 7.

The data here presented show an inverse relationship between the glucose concentration in the medium and the cell viability in the presence of H_2O_2 and the analyses performed using GOxBrcS-SPE sensor (Figure 7B and D) were comparable to the GOx-SPE sensor (Figure 7A and C). The little differences of measurement were probably due to the liquid diffusion and to the different GOx accessibility in a 3D-structure as well as GOxBrcS-SPE sensor.

Therefore, these results open the way for studying the cellular behavior using not invasive and not expensive vegetable biosensors by direct analysis of the cell culture medium. Moreover, BrcS as plant-derived biomaterial could have several advantages including biocompatibility, microporosity, xeno-free plant-derived properties, easy handling and low cost for 3D -cell culture systems fabrication.

3.7 BrcS for stem cell growth

Stem cell models are being adopted by the pharmaceutical industry for preclinical toxicity studies [41–43]. The availability and reproducibility of stem cells make them useful sources for *in vitro* toxicity test models in toxicology and pharmaceutical production. In this context, we investigated on the cell scaffolding properties of BrcS for 3D- cMSC cultures. Several studies have demonstrated that the micro-porosity of biomaterial is an important characteristic for a good scaffolding property for tissue regeneration. An adequate sized opening could allow a good cellular proliferation and vascular ingrowth, for carrying nutrients and oxygen. [44] Therefore, the observed

micro-porosity of BrcS can be an important characteristic for improving the cell proliferation in a 3D culture system. cMSC were seeded on BrcS that were pre-conditioned with DMEM for two weeks in sterile conditions. After 4 weeks of cell growth the cell viability was evaluated by WST-1 assay (Figure 9A and B) demonstrating the presence of cells with active metabolism. In the Figure 9C are shown the fluorescence micrographs obtained by confocal microscopy and z-stack imaging. Hoechst staining of the nuclei did not show pyknosis (see Figures 9D) and the cells were widely distributed into the scaffold (Figure 9C).

Moreover, the expression of α-Sma was analysed after two weeks of cell growth onto BrcS by immunostaining using anti α-Sma antibody. In the Figure 8E are shown fluorescence micrographs after Hoechst *in vivo* staining and Ab-α-Sma detection by 488-Alexa fluorochrome-conjugated secondary antibody. Although the presence of the α-Sma should be better investigated by western blotting, this preliminary analysis suggests a potential effect of the BrcS scaffold on the commitment of a differentiation process on the cMSCs into muscle cells. This could be related to the stiffness of the cellulosic BrcS that could give the right physical stimuli for an initial myo-differentiation process. Other studies are in progress in order to better demonstrate this property of BrcS.

Recently, decellularized apple-derived scaffolds, with pores of ~200 μm in diameter, has been applied for culturing and osteoblastic differentiation of human mesenchymal stem cells and iPSCs. [12,14,15] In these studies, the clinical prospectives, using resultant organoids as biocompatible *in vivo* implants in the 3D engineering of bone were explored. Unclearly, in a recent study other plant-derived scaffolds, including broccoli, were not suitable for the culturing of iPSCs. By contrast, here we demonstrated that after pre-conditioning of BrcS with cell culture medium BrcS was able to support the cell-attachment and growth of cMSC. The sustainable use of vegetable waste scaffolds (VWS) opens the possibility to explore not only a plethora of different 3D-microstructures on the stem cell growth and differentiation, but also potential effects of different chemical composition of cellulose tissues with micro-amount of natural organo-compounds, such as organo sulphur compounds, polyphenols etc. that are usually present in the plants.

Our results demonstrate that the micro-structured BrcS could have a scaffolding property for realizing easy handling and low-cost optical/electrochemical biosensors, able to integrate mesenchymal stem cells and to create a working sensor and/or

diagnostic device for monitoring the reactivity of the cells in the presence of chemical / biological toxic agents.

4. Conclusions

Biosensors have successfully demonstrated their capability to monitor different environmental and food contaminants, also proving their usefulness in clinical diagnosis with the most successful device being the electrochemical biosensor for blood glucose based on glucose oxidase. [45,46] Here GOxBrcS-SPE was proposed as an example of a low-cost biosensor using 3D structure for the immobilization of the glucose oxidase enzyme, showing great performance compared to the traditional GOx-SPE biosensor. Although the waste cellulose lacks fine control over the physical and biochemical properties of the scaffold, it results in an easily obtainable natural derived with micro-porous structure. BrcS are porous enough to allow for efficient nutrients/gas exchange, biocompatible, easily functionalized, also with enzymes, and useful for the sponge-like property. Moreover, a good growth of cMSC onto BrcS was observed suggesting that GOxBrcS-SPE/MSCs systems could have several important applications including: screening of drugs libraries, toxicology as well as environmental and food analyses.

A potential myo-commitment of the cMSC cultured onto BrcS was also observed opening the way to potential applications of MSC-BrcS systems for the fabrication of cell-based biosensors and low-cost lab-on-chip systems. Moreover, MSC-BrcS systems could find application in a new branch of food industry, such as the production of novel and less expensive type of *in vitro* meat, where the muscle differentiation of MSC and the vegetable fiber could be combined.

Supplementary Materials: Figures 1S -4S

Abbreviations: 3D, three-dimensional; ATR-FTIR, Attenuated total reflection Fourier transform infrared spectroscopy; Brc, stalk of broccoli; BrcS, 3D-scaffolds ; BrcS-SPE, BrcS-screen printed electrode biosensor; cMSC human Lin^- $Sca\text{-}1^{pos}$ cardiac mesenchymal cells; cMSC, human cardiac mesenchymal stem cells; Cyclic voltammetry CV; D_0 diffusion coefficient; D_0 diffusion coefficient; D_A Anodic diffusion coefficients; DMEM Dulbecco's Modified Eagle Medium; D_R Cathodic diffusion coefficients; ECM, extracellular matrix; EDX Energy-dispersive X-ray spectroscopy; GOx, Glucose oxidase; GOx-SPE, Glucose oxidase screen printed electrode biosensor GOxBrcS-SPE sensor, Glucose oxidase/3D-scaffold- screen printed electrode biosensor; iPSCs, Induced pluripotent stem cells; LOD, detection limit; NHDF, human dermal fibroblast; OSCs, organosulfur compounds; PFA, paraformaldehyde; R.T., scaffold rehydration time; SDS, sodium dodecyl sulfate; S.D.T., scaffold dehydration time; SEM, Scanning Electron Microscopy; SPE, screen printed electrode biosensor; sulphur S;VW, Vegetable wastes; WR working range; WST-1 assay, Water-Soluble Tetrazolium salt assay; WU, water uptake; α-Sma, α-smooth muscle actin

Acknowledgments: We thank Silvia Buonvino for the critical discussion of the results, P. Di Nardo to give us the Lin^- $Sca\text{-}1^+$ human cardiac MSC line, and E. Di Bartolomeo for using the SEM facility of the University of Rome Tor Vergata.

Conflicts of Interest: The authors declare no conflict of interest.

References

[1] L.G. Griffith, M.A. Swartz, Capturing complex 3D tissue physiology in vitro, Nat Rev Mol Cell Biol. 7 (2006) 211–224. https://doi.org/10.1038/nrm1858.

[2] J.R. Gershlak, S. Hernandez, G. Fontana, L.R. Perreault, K.J. Hansen, S.A. Larson, B.Y.K. Binder, D.M. Dolivo, T. Yang, T. Dominko, M.W. Rolle, P.J. Weathers, F. Medina-Bolivar, C.L. Cramer, W.L. Murphy, G.R. Gaudette, Crossing kingdoms: Using decellularized plants as perfusable tissue engineering scaffolds, Biomaterials. 125 (2017) 13–22. https://doi.org/10.1016/j.biomaterials.2017.02.011.

[3] R.A. Terry, J.M.A. Tilley, G.E. Outen, Effect of pH on cellulose digestion underin vitro conditions, J. Sci. Food Agric. 20 (1969) 317–320. https://doi.org/10.1002/jsfa.2740200514.

[4] P. Benya, Dedifferentiated chondrocytes reexpress the differentiated collagen phenotype when cultured in agarose gels, Cell. 30 (1982) 215–224. https://doi.org/10.1016/0092-8674(82)90027-7.

[5] D. Klemm, D. Schumann, U. Udhardt, S. Marsch, Bacterial synthesized cellulose — artificial blood vessels for microsurgery, Progress in Polymer Science. 26 (2001) 1561–1603. https://doi.org/10.1016/S0079-6700(01)00021-1.

[6] A. Svensson, E. Nicklasson, T. Harrah, B. Panilaitis, D.L. Kaplan, M. Brittberg, P. Gatenholm, Bacterial cellulose as a potential scaffold for tissue engineering of cartilage, Biomaterials. 26 (2005) 419–431. https://doi.org/10.1016/j.biomaterials.2004.02.049.

[7] H. Page, P. Flood, E.G. Reynaud, Three-dimensional tissue cultures: current trends and beyond, Cell Tissue Res. 352 (2013) 123–131. https://doi.org/10.1007/s00441-012-1441-5.

[8] W. Czaja, A. Krystynowicz, S. Bielecki, R. Brownjr, Microbial cellulose—the natural power to heal wounds, Biomaterials. 27 (2006) 145–151. https://doi.org/10.1016/j.biomaterials.2005.07.035.

[9] N.O. Gomes, E. Carrilho, S.A.S. Machado, L.F. Sgobbi, Bacterial cellulose-based electrochemical sensing platform: A smart material for miniaturized biosensors, Electrochimica Acta. 349 (2020) 136341. https://doi.org/10.1016/j.electacta.2020.136341.

[10] W.K. Czaja, D.J. Young, M. Kawecki, R.M. Brown, The Future Prospects of Microbial Cellulose in Biomedical Applications, Biomacromolecules. 8 (2007) 1–12. https://doi.org/10.1021/bm060620d.

[11] J. Kucińska-Lipka, I. Gubanska, H. Janik, Bacterial cellulose in the field of wound healing and regenerative medicine of skin: recent trends and future prospectives, Polym. Bull. 72 (2015) 2399–2419. https://doi.org/10.1007/s00289-015-1407-3.

[12] D.J. Modulevsky, C. Lefebvre, K. Haase, Z. Al-Rekabi, A.E. Pelling, Apple Derived Cellulose Scaffolds for 3D Mammalian Cell Culture, PLoS ONE. 9 (2014) e97835. https://doi.org/10.1371/journal.pone.0097835.

[13] D.J. Modulevsky, C.M. Cuerrier, A.E. Pelling, Biocompatibility of Subcutaneously Implanted Plant-Derived Cellulose Biomaterials, PLoS ONE. 11 (2016) e0157894. https://doi.org/10.1371/journal.pone.0157894.

[14] C. Demitri, M.G. Raucci, A. Giuri, V.M. De Benedictis, D. Giugliano, P. Calcagnile, A. Sannino, L. Ambrosio, Cellulose-based porous scaffold for bone tissue engineering applications: Assessment of hMSC proliferation and

differentiation: Cellulose-Based Porous Scaffold for Bone Tissue Engineering Applications, J. Biomed. Mater. Res. 104 (2016) 726–733. https://doi.org/10.1002/jbm.a.35611.

[15] J. Lee, H. Jung, N. Park, S.-H. Park, J.H. Ju, Induced Osteogenesis in Plants Decellularized Scaffolds, Sci Rep. 9 (2019) 20194. https://doi.org/10.1038/s41598-019-56651-0.

[16] M.L. Latour, M. Tarar, R.J. Hickey, C.M. Cuerrier, I. Catelas, A.E. Pelling, Plant-derived Cellulose Scaffolds for Bone Tissue Engineering, Bioengineering, 2020. https://doi.org/10.1101/2020.01.15.906677.

[17] D. Huh, G.A. Hamilton, D.E. Ingber, From 3D cell culture to organs-on-chips, Trends in Cell Biology. 21 (2011) 745–754. https://doi.org/10.1016/j.tcb.2011.09.005.

[18] Y. Pan, N. Hu, X. Wei, L. Gong, B. Zhang, H. Wan, P. Wang, 3D cell-based biosensor for cell viability and drug assessment by 3D electric cell/matrigel-substrate impedance sensing, Biosensors and Bioelectronics. 130 (2019) 344–351. https://doi.org/10.1016/j.bios.2018.09.046.

[19] P.S. Sfragano, S. Laschi, I. Palchetti, Sustainable Printed Electrochemical Platforms for Greener Analytics, Front. Chem. 8 (2020) 644. https://doi.org/10.3389/fchem.2020.00644.

[20] N. Duraipandy, R. Lakra, K. Vinjimur Srivatsan, U. Ramamoorthy, P.S. Korrapati, M.S. Kiran, Plumbagin caged silver nanoparticle stabilized collagen scaffold for wound dressing, J. Mater. Chem. B. 3 (2015) 1415–1425. https://doi.org/10.1039/C4TB01791A.

[21] M. Ciocci, I. Cacciotti, D. Seliktar, S. Melino, Injectable silk fibroin hydrogels functionalized with microspheres as adult stem cells-carrier systems, International Journal of Biological Macromolecules. 108 (2018) 960–971. https://doi.org/10.1016/j.ijbiomac.2017.11.013.

[22] F. Ricci, D. Moscone, C.S. Tuta, G. Palleschi, A. Amine, A. Poscia, F. Valgimigli, D. Messeri, Novel planar glucose biosensors for continuous monitoring use, Biosensors and Bioelectronics. 20 (2005) 1993–2000. https://doi.org/10.1016/j.bios.2004.09.010.

[23] A.J. Bard, L.R. Faulkner, Electrochemical methods: fundamentals and applications, 2nd ed, Wiley, New York, 2001.

[24] R. Cancelliere, K. Carbone, M. Pagano, I. Cacciotti, L. Micheli, Biochar from Brewers' Spent Grain: A Green and Low-Cost Smart Material to Modify Screen-Printed Electrodes, Biosensors. 9 (2019) 139. https://doi.org/10.3390/bios9040139.

[25] A.M. Smits, P. van Vliet, C.H. Metz, T. Korfage, J.P. Sluijter, P.A. Doevendans, M.-J. Goumans, Human cardiomyocyte progenitor cells differentiate into functional mature cardiomyocytes: an in vitro model for studying human cardiac physiology and pathophysiology, Nat Protoc. 4 (2009) 232–243. https://doi.org/10.1038/nprot.2008.229.

[26] G. Forte, S. Pietronave, G. Nardone, A. Zamperone, E. Magnani, S. Pagliari, F. Pagliari, C. Giacinti, C. Nicoletti, A. Musaró, M. Rinaldi, M. Ribezzo, C. Comoglio, E. Traversa, T. Okano, M. Minieri, M. Prat, P. Di Nardo, Human Cardiac Progenitor Cell Grafts as Unrestricted Source of Supernumerary Cardiac Cells in Healthy Murine Hearts, STEM CELLS. 29 (2011) 2051–2061. https://doi.org/10.1002/stem.763.

[27] M. Koyanagi, S. Kawakabe, Y. Arimura, A comparative study of colorimetric cell proliferation assays in immune cells, Cytotechnology. 68 (2016) 1489–1498. https://doi.org/10.1007/s10616-015-9909-2.

[28] D.-W. Kim, Y.-K. Sun, Electrochemical characterization of gel polymer electrolytes prepared with porous membranes, Journal of Power Sources. 102 (2001) 41–45. https://doi.org/10.1016/S0378-7753(01)00771-6.

[29] D.A. Moreno, M. Carvajal, C. López-Berenguer, C. García-Viguera, Chemical and biological characterisation of nutraceutical compounds of broccoli, Journal of Pharmaceutical and Biomedical Analysis. 41 (2006) 1508–1522. https://doi.org/10.1016/j.jpba.2006.04.003.

[30] P.K. Revelou, M.G. Kokotou, C.S. Pappas, V. Constantinou-Kokotou, Direct determination of total isothiocyanate content in broccoli using attenuated total reflectance infrared Fourier transform spectroscopy, Journal of Food Composition and Analysis. 61 (2017) 47–51. https://doi.org/10.1016/j.jfca.2017.01.020.

[31] Z. Movasaghi, S. Rehman, Dr.I. ur Rehman, Fourier Transform Infrared (FTIR) Spectroscopy of Biological Tissues, Applied Spectroscopy Reviews. 43 (2008) 134–179. https://doi.org/10.1080/05704920701829043.

[32] E. Niranjana, B.E. Kumara Swamy, R. Raghavendra Naik, B.S. Sherigara, H. Jayadevappa, Electrochemical investigations of potassium ferricyanide and dopamine by sodium dodecyl sulphate modified carbon paste electrode: A cyclic voltammetric study, Journal of Electroanalytical Chemistry. 631 (2009) 1–9. https://doi.org/10.1016/j.jelechem.2009.02.011.

[33] M. Mayyas, V. Sahajwalla, Carbon nano-sponge with enhanced electrochemical properties: A new understanding of carbon activation, Chemical Engineering Journal. 358 (2019) 980–991. https://doi.org/10.1016/j.cej.2018.10.094.

[34] J. Billen, P. Gzil, N. Vervoort, G.V. Baron, G. Desmet, Influence of the packing heterogeneity on the performance of liquid chromatography supports, Journal of Chromatography A. 1073 (2005) 53–61. https://doi.org/10.1016/j.chroma.2004.10.042.

[35] A. García-Miranda Ferrari, C. Foster, P. Kelly, D. Brownson, C. Banks, Determination of the Electrochemical Area of Screen-Printed Electrochemical Sensing Platforms, Biosensors. 8 (2018) 53. https://doi.org/10.3390/bios8020053.

[36] Nakoryakov, V. E., & Gasenko, V. G. (2006). Effect of the capillary forces in porous electrodes on the voltage-current characteristic of polymer electrolyte membrane fuel cells. Theoretical Foundations of Chemical Engineering, 40(2), 116–125. doi:10.1134/s0040579506020035

[37] A. Memoli, M.C. Annesini, M. Mascini, S. Papale, S. Petralito, A comparison between different immobilised glucoseoxidase-based electrodes, Journal of Pharmaceutical and Biomedical Analysis. 29 (2002) 1045–1052. https://doi.org/10.1016/S0731-7085(02)00145-0.

[38] S.J. Konopka, Bruce. McDuffie, Diffusion coefficients of ferri- and ferrocyanide ions in aqueous media, using twin-electrode thin-layer electrochemistry, Anal. Chem. 42 (1970) 1741–1746. https://doi.org/10.1021/ac50160a042.

[39] A.A. Karyakin, O.V. Gitelmacher, E.E. Karyakina, Prussian Blue-Based First-Generation Biosensor. A Sensitive Amperometric Electrode for Glucose, Anal. Chem. 67 (1995) 2419–2423. https://doi.org/10.1021/ac00110a016.

[40] B.I. Kurganov, A.V. Lobanov, I.A. Borisov, A.N. Reshetilov, Criterion for Hill equation validity for description of biosensor calibration curves, Analytica

Chimica Acta. 427 (2001) 11–19. https://doi.org/10.1016/S0003-2670(00)01167-3.

[41] P. Rana, B. Anson, S. Engle, Y. Will, Characterization of Human-Induced Pluripotent Stem Cell–Derived Cardiomyocytes: Bioenergetics and Utilization in Safety Screening, Toxicological Sciences. 130 (2012) 117–131. https://doi.org/10.1093/toxsci/kfs233.

[42] J.G. Reynolds, E. Geretti, B.S. Hendriks, H. Lee, S.C. Leonard, S.G. Klinz, C.O. Noble, P.B. Lücker, P.W. Zandstra, D.C. Drummond, K.J. Olivier, U.B. Nielsen, C. Niyikiza, S.V. Agresta, T.J. Wickham, HER2-targeted liposomal doxorubicin displays enhanced anti-tumorigenic effects without associated cardiotoxicity, Toxicology and Applied Pharmacology. 262 (2012) 1–10. https://doi.org/10.1016/j.taap.2012.04.008.

[43] H.C. Ott, T.S. Matthiesen, S.-K. Goh, L.D. Black, S.M. Kren, T.I. Netoff, D.A. Taylor, Perfusion-decellularized matrix: using nature's platform to engineer a bioartificial heart, Nat Med. 14 (2008) 213–221. https://doi.org/10.1038/nm1684.

[44] S. Saravanan, R.S. Leena, N. Selvamurugan, Chitosan based biocomposite scaffolds for bone tissue engineering, International Journal of Biological Macromolecules. 93 (2016) 1354–1365. https://doi.org/10.1016/j.ijbiomac.2016.01.112.

[45] S. Kröger, S. Piletsky, A.P.F. Turner, Biosensors for marine pollution research, monitoring and control, Marine Pollution Bulletin. 45 (2002) 24–34. https://doi.org/10.1016/S0025-326X(01)00309-5.

[46] D.R. Thévenot, K. Toth, R.A. Durst, G.S. Wilson, Electrochemical biosensors: recommended definitions and classification1International Union of Pure and Applied Chemistry: Physical Chemistry Division, Commission I.7 (Biophysical Chemistry); Analytical Chemistry Division, Commission V.5 (Electroanalytical Chemistry).1, Biosensors and Bioelectronics. 16 (2001) 121–131. https://doi.org/10.1016/S0956-5663(01)00115-4.

Table 1: CV studies of BrcS stove's residence (S. R.) time electrochemical characterization: peaks current (Ipa/pc) and redox potentials obtained using 20mM Potassium Ferricyanide in 50 mM phosphate buffer ,pH 7.4, with 10 mM KCl,

S. D. Times (min.)	Ipa (µA)	Ipc (µA)	ΔI (µA)	Epa (Volt)	Epc (Volt)	ΔE
60	231 ± 9	-217 ± 11	448 ± 10	304 ± 6	83 ± 6	221 ± 6
120	394 ± 14	-378 ± 16	772 ± 15	304 ± 8	83 ± 5	221 ± 7
180	156 ± 11	-122 ± 13	278 ± 12	314 ± 7	53 ± 7	261 ± 7

Table 2: Diffusion coefficient (D_0) calculation: Brc-SPE in 5 mM Potassium Ferricyanide 100 mM KCl solution a scan rate of 0.03 Vs^{-1}.

Scan Rates (Vs^{-1})	Anodic D_0 (cm^2s^{-1})	Cathodic D_0 (cm^2s^{-1})	Anodic $\bar{D}_0$ (cm^2s^{-1})	Cathodic $\bar{D}_0$ (cm^2s^{-1})
0.03	$(1.34 \pm 0.12)\cdot 10^{-7}$	$(9.55 \pm 0.10)\cdot 10^{-8}$	$(1.28 \pm 0.13)\cdot 10^{-7}$	$(1.04 \pm 0.11)\cdot 10^{-7}$

Table 3: Linear Range, limit of detection and relative standard deviation (RSD) calculated for the different glucose sensors.

Biosensor	Linear Range (µM)	LOD (µM)	RSD%
GOx/BrcS-SPE	0.05 - 0.5	16	8
GOx-SPE	0.05 - 1.0	12	7

Figure Captions

Figure 1. Schematization of Enzyme/BrcS-SPE preparation steps. **a)** BrcS hydration using a solution of distilled water with GOx ($10 mgmL^{-1}$), Nafion (2%), Glutaraldehyde (10%) and BSA (5%); **b)** GOx-BrcS positioning on PB-SPE and c) platforms dehydration (37°C, 2hours); **d)** rehydration using different concentration of glucose solution and **e**) electrochemical measurement (Amperometry, using 50 mV potential for 300s), respectively.

Figure 2. Ultrastructural Characterization with Scan Electron Microscopy (SEM) at different magnifications (**A**) at 1K (a) (scale bar 20 μm), 2K (b), 5K (c) and (**B**) 3K (scale bars 10 μm); (**C**) Energy-dispersive X-ray spectroscopy (EDX) of BrcS.

Figure 3. BrcS characterization**. A**) Fourier transform infrared (FTIR) spectra of decellularized broccoli tissues; **B**) Digital image of the BrcS before and after hydration; **C**) % water uptake. The bars indicate the SD.

Figure 4. Electrochemical characterization of BrcS-SPE. Cyclic voltamogramms in 50 mM Phosphate Buffer, pH 7.4, with 10 mM KCl, of: **A**) BrcS-SPE; **B**) Brc-SPE for different stove's residence time (S.R.), (n = 10, RSD 6%); **C**) BrcS-SPE for different rehydration time (R.T.). Potential scan rate: 30 mVs^{-1}; **D**) study of different scan rates ($mV \cdot S^{-1}$) using 5 mM Potassium Ferricyanide with BrcS/SPE.

Figure 5. Electrochemical characterization of GOxSPE and GOx/BrcS-SPE. **A**) Calibration curve between the cathodic current and the concentration of glucose in 50 mM phosphate buffer, pH7.4, 10 mM KCl) obtained with GOx-SPE (• red) and GOx/BrcS-SPE (• blue) biosensor (insert: linear range); **B**) Lineweaver–Burk plot of GOx-SPE (• red) and GOx/BrcS-SPE (• blue) biosensor.

Figure 6. GOx/BrcS-SPE as biosensor for cellular glucose uptake. Analysis of glucose concentration expressed in faradic current in the culture media performed using **A**) GOx-SPE and **B**) GOx/BrcS-SPE. Blank corresponds to the electrochemical measure of the concentration of glucose in the medium without cells, cMSC and

NHDF are the culture media after 3 days of cell growth of cMSC and NHDF, respectively. $^{*}p$ value < 0.05. The measures were the results of 3 independents experiments.

Figure 7. GOx/BrcS-SPE as biosensor for cell growth. Representative micrographs of cMSC (seeded at a cell density of $20x10^3$ cells/cm^2) after 12 h of growth in the absence **A**) and in the presence **B**) of 100 μM H_2O_2 after 12 (a and b) and 24 h (c and d) of growth. Scale bars are 100 and 50 μm, Mag. 10X (a and c) and 20X (b and d)**.** Electrochemical measurements of cell culture media by GOx- **(C** and **E)** and GOx/BrcS-SPE **(D** and **F)** biosensors after treatment of cMSC **(C** and **D)** and NHDF **(E** and **F)** in the presence of 100 μM H_2O_2 (cMSC+H_2O_2; NHDF+H_2O_2) (cell seeding at cell density of $20x10^3$ cells/cm^2). cMSC and NHDF correspond to the analyses of the media of the controls after 12 h, cMSC or/NHDF growth in the absence of H_2O_2. Blank is the analysis of the DMEM medium without cells. $^{****}p$ value < 0.0001. The measures were the results of 3 independents experiments.

Figure 8. BrcS as 3D-scaffold for stem cells growth. **C**) Confocal laser scanning micrographs of cMSCs cultured for four weeks into BrcS (z-stack of 41 focal planes). F-actin was stained with Alexa-fluor 568 phalloidin-conjugate (in red) and the nuclei were stained using Hoechst 33342 (in blue) at 20X and **D**) at 40X of magnification, z-stack of 31 focal planes. Scale bars = 50 and 20 μm **E**) Fluorescence micrographs of cMSC after two weeks of growth on BrcS. Hoechst *in vivo* staining and 488-Alexa fluorochrome-conjugated secondary antibody detection of α-Sma antibody at 50X of magnification, scale bars=10 μm; **F**) phase contrast (a) and fluorescence (b) micrographs of the scaffold with cells after two weeks of growth at 20X of magnification and the merged image (c). Scale bars = 20 μm.

Vegetable waste Scaffolds for 3D-stem cell proliferating systems and low cost Biosensors

Rocco Cancelliere[1], Francesca Zurlo[1], Laura Micheli[1&]* and Sonia Melino[1,2&]*

[1.]Department of Chemical Science and Technologies, University of Rome "Tor Vergata", via della Ricerca Scientifica 1, 00133-Rome, Italy;
[2]CIMER Center for Regenerative Medicine, University of Rome Tor Vergata, via Montpellier 1, 0166-Rome, Italy;
[&]These authors contributed equally to the work
* Correspondence: Sonia Melino e-mail: melinos@uniroma2.it; Laura Micheli e-mail: laura.micheli@uniroma2.it; Tel. #39-067259-4410/4420;

Highlights

- 3D-enzyme biosensor development by vegetable wastes
- Production of a 3D vegetable derived scaffold for cell proliferation analysis
- 3D sponge like scaffolds derived from broccoli for 3D-stem cell growth